Microchimica Acta (2019) 186:616
https://doi.org/10.1007/s00604-019-3740-y

ORIGINAL PAPER

Amperometric enzymatic sensing of glucose using porous carbon nanotube films soaked with glucose oxidase

Waraporn Rernglit[1] · Somjai Teanphonkrang[2] · Wipa Suginta[1,2] · Albert Schulte[2]

Received: 22 February 2019 / Accepted: 3 August 2019

Abstract

Glucose oxidase was soaked into a porous carbon nanotube film coating on a platinum disk electrode, then trapped beneath a topcoat of electrodeposition paint. The resulting sensors, operated at a potential of +0.6 V (*vs*. Ag/AgCl), produced a glucose signal that was linear up to 40 mM, with a 50 μM detection limit. Signal stability over >100 h of continuous operation in a flow cell showed the remarkable functional durability of the biosensor, and confirmed that the electropaint coating effectively prevented loss of the enzyme. This performance is deemed to derive from the minimalistic immobilization layer design and the prevention of protein leakage. The immobilization method has a potentially wide scope, in that it may also be applicable in other types of enzymatic biosensor.

Keywords Biosensors · Nanomaterials · Immobilization · Amperometry · Electrodeposition paint

Introduction

Substrate-specific electrochemical biosensors are important analytical tools in medical analysis, the biotech/pharma industries and environmental test centers. The most widely used is the glucose oxidase (GOx)-based glucose biosensor [1, 2], which in mass-produced, screen-printed electrode format has long served in hand-held electronic devices for blood glucose assays in the home, by persons with diabetes or hypoglycemia. However, with suitable alternative protein biocatalysts, not only glucose but also many other species are measurable, the reviewed electrochemical biosensing of pesticides, galactose, bilubirin and ethanol being examples of successful designs [3–6].

The ongoing aims of biosensor makers are enhance analytical performance, simplification of fabrication and miniaturization. Routes to high sensitivity, long-term response stability and long service-life of enzyme electrodes involve adaptations of the entire sensor design, including modification of the protein immobilization matrix, configuration of signal transduction and choice and chemical pre-modification of carrier electrode structures. In optimizing the immobilization layer, the integration of nano-materials of high catalytic activity, large surface area and unique electronic features became a prime strategy in achieving advanced analytical figures of merit [7–9]. In fact, metal and metal oxide nanoparticles and wires, semiconductor quantum dots, advanced graphitic materials such as fullerenes and carbon nanotubes (CNTs) and layered nanosheets of graphene, graphene oxide or transition metal di-chalcogenides have all been tested as functional sensor components. Functioning enzyme biosensors with CNT-based immobilization have mostly involved matrix fusions with other nano-materials such as nanoscale natural or synthetic polymers, silicon dioxide sol-gel nanostructures, synthetic redox nanoparticles and nano-catalysts [10–20]; however, construction and success depend on the availability of special raw materials and/or multiple assembly steps. Obviously, these constraints make electrode production for routine usage by potential end-users difficult and the manufacture of mass quantities for widespread application

Electronic supplementary material The online version of this article (https://doi.org/10.1007/s00604-019-3740-y) contains supplementary material, which is available to authorized users.

✉ Wipa Suginta
wipa.s@vistec.ac.th

✉ Albert Schulte
albert.s@vistec.ac.th

[1] School of Chemistry, Institute of Science, Suranaree University of Technology (SUT), Nakhon Ratchasima 30000, Thailand

[2] School of Biomolecular Science and Engineering (BSE), Vidyasirimedhi Institute of Science and Technology (VISTEC), Wangchan Valley, Rayong 21210, Thailand

Published online: 13 August 2019

problematic. The few reported glucose oxidase biosensors with pure CNT immobilization layers detected the analyte at μM levels but had limited linear ranges of the order of just a few mM [21–26], while those that combined μM detection limits with wide linear ranges involved specially modified CNTs [27].

The present study produced systematic evidence that biosensors with the signaling biocatalyst entrapped in simple films of single-walled CNTs are competitive with equivalent probes with sensing layers composed of more complex CNT/nanomaterial composites. Using amperometric glucose biosensing as a model, detailed calibration, response time, detection limit and response stability tests, along with model sample recovery rate trials and glucose analysis in human serum, were conducted to assess analytical performance with a simple CNT-based sensor architecture. CNT/GOx layer formation relied on simple manual drop-and-dry steps, with commercial electrodeposition paint (EDP) [28] forming a final coating that allowed glucose and oxygen diffusion to entrapped GOx while preventing protein leakage. A key advantage of this sensor design is its ease of construction, together with the wide dynamic range for glucose assays, low-μM practical detection limit and long-term response stability. Another asset is that this design is suitable for automated mass production of enzyme biosensors, from commercially available 'ready-to-go' starting materials.

Experimental section

Chemicals and materials

Glucose oxidase (GOx, EC 1.1.3.4, from *Aspergillus niger*) was from S.M. Chemical Supplies Co., Ltd. (Bangkok, Thailand, https://www.smchem.co.th) as a product of Sigma-Aldrich® (St. Louis, MO, USA, https://www.sigmaaldrich.com, product no. G1741, lyophilized, 75% protein, 136,300 units/g). Anhydrous D (+) glucose, from Italmar (Thailand) Co., Ltd. (Bangkok, Thailand, http://www.italmarth.com), was a product of CARLO ERBA Reagents S.A.S. (Val-de-Reuil, France, https://www.carloerbareagents.com). Purified carboxylated single-walled CNTs, with 1.0–3.0 at-% carboxylic acid entities, were from Carbon Solutions, Inc. (Riverside, CA, USA, www.carbonsolution.com). The commercial cathodic electrodeposition paint (EDP) Clearclad® was a kind gift for research purposes from LHV Coatings Ltd. (Birmingham, England, www.lvh-coatings.com). All other chemicals were Sigma-Aldrich® analytical grade products. Ultrapure de-ionized water was used for aqueous solution preparation. Unless otherwise specified the electrolyte in biosensor tests was 0.1 M sodium phosphate buffer, supplemented with 100 mM KCl and adjusted to pH 7.0.

Instrumentation

Cyclic voltammetry with unmodified and CNT-modified 3-mm-diameter Pt disc electrodes and amperometry with CNT/GOx/EDP-modified 3-mm-diameter Pt- or Au-disk biosensors were carried out with a Reference 600® potentiostat from Gamry Instruments Inc. (Warminster, PA, USA, www.gamry.com). Pt and Ag/AgCl wires served as the counter- (CE) and pseudo reference-electrode (RE), respectively. For long-term response tests the gold disk versions of the biosensors were used in an electrochemical flow cell, run by the EA163/ED410 potentiostat/e-corder system from eDAQ Pty. Ltd. (Denistone East, Australia, www.edaq.com). The RE in the flow system was a fritted Ag/AgCl (3 M KCl) electrode while the tubular stainless-steel cell outlet formed the CE. The flow of electrolyte with or without glucose was controlled at about 20 μL s^{-1} by a peristaltic pump (Minipuls-3® from Gilson, Middleton, WI, USA, gilson.com/system-minipuls-3-peristaltic-pumps.html).

Biosensor fabrication

Commercial 3-mm-diameter Pt disk electrodes from Gamry Instruments Inc. with a Kel-F® body and an outer diameter of 7 mm were polished on a soft textile pad soaked in alumina slurry, first of 5 μm and then 1 μm particle size. After removal of the polishing paste by ultra-sonication and rinsing, electrodes were air-dried at room temperature (RT). A 5.0 μL drop of a suspension of 5.0 mg CNTs in 1 mL H_2O was then placed on the smooth Pt disk and allowed to dry. Three repetitions of this CNT drop coating step resulted in the formation of a thin film of the black graphitic nanomaterial on the noble metal surface. Next, a 5.0 μL drop of a 5.0 mg mL^{-1} solution of GOx in H_2O was placed on the dried CNT deposit; this step was repeated twice, with subsequent solvent evaporation at room temperature. Finally, the addition of a thin polymer cover to the CNT/GOx deposit was achieved in a two-electrode cell with a Pt wire counter- electrode, by a 2 min-long deposition of the cathodic electropaint at a potential of - 3.5 V. After 30 min stirring at moderate speed in 0.1 M phosphate/KCl, pH 7.0, the CNT/GOx/EDP glucose biosensor discs were stored at 4 °C in the buffered solution. A similar procedure was used for tuning 3-mm-diameter Au disk electrodes into glucose biosensors.

Biosensor application for glucose determination in serum

The blood sample for serum preparation was an agreed donation of the principal investigator of study (AS) and analyzed for the glucose content by the Clinical Laboratory of the Suranaree University of Technology, Nakhon Ratchasima, Thailand. For all serum glucose measurements a thin Nafion

layer was placed over the CNT/GOx/EDP immobilization layer, as a barrier against interference by ascorbate and/or urate [12]. To establish this layer, 5 μL of a 10% Nafion solution were dropped on the disc face of a pre-modified electrode and allowed to dry at room temperature for film formation. While not in use, CNT/GOx/EDP/Nafion glucose biosensors were stored at 4 °C in 0.1 M phosphate/KCl, pH 7.0.

Results and discussion

Nanoporous sponge character of the biosensor facade

Freshly polished 3-mm-diameter Pt disk electrodes with a mirror-like surface appearance (Fig. 1A-a) were modified with pure CNT deposits and then modified with GOx. Functional biosensor surface modification involved a sequence of two manual drop-and-dry casting steps, first with a suspension of carboxylated CNTs in water (Fig. 1A-b, left) and then with an aqueous GOx solution (Fig. 1A-c, left). In the first step an even, strongly adhering spongy network of CNT filaments (Fig. 1A-b, right & B-a) was formed on the polished Pt disk; these are electrically chain-wired to each other and to the Pt surface, which is important for efficient signal generation (i.e. anodic H_2O_2 detection).

SEM examination revealed abundant, irregularly distributed nanopores in the CNT deposit (Fig. 1B-b), while cyclic voltammetry in pure 0.1 M KCl confirmed the large surface area of the spongy Pt disk adaptation, resulting in large capacitance currents (Supplementary Fig. S1). In the second step, application of drops of GOx stock and subsequent solvent evaporation loaded the nanopores of the CNT layer with protein. Firmly attached CNT/GOx (Fig. 1A-c, right) was finally over-coated with cathodic EDP paint (Fig. 1A-d). The polymer cover was conveniently formed in a 2-electrode cell, in which CNT/GOx-covered Pt disks and a coiled Pt wire were coupled to the negative and positive terminals, respectively, of a laboratory power supply. During sensor use and storage in aqueous buffers the EDP coating prevented escape of trapped GOx molecules from the CNT sponge, guaranteeing good sensor response stability.

Sensor performance and calibration

In their conventional amperometric calibration trials (CNT/GOx)/EDP-Pt biosensors showed reasonably fast response times, adequate sensitivity and a proportional signal over a wide range of analyte concentrations. Figure 2a is a typical amperometric recording of a CNT/GOx/EDP-modified Pt-disk electrode during successive additions of small aliquots of glucose stock solution. It shows a series of well-defined steps in the anodic H_2O_2 current trace on titration with glucose solution, with approximately 10 s needed to reach 90% of the final steady-state signal (Fig. 2b plus inset).

Figure 2c is the calibration plot derived from the amperogram in Fig. 2a, and shows a plateau current, i_{max}, of 27 μA, a linear response up to 60 mM glucose ($r^2 = 0.992$) and a sensitivity of 0.35 μA mM^{-1} (4.9 μA mM^{-1} cm^{-2}, normalized to the geometric surface area of the Pt disk transducer). For 12 identically prepared biosensors the mean values and standard deviations for i_{max}, linear response range width and sensitivity were 28.0 ± 8.1 μA, 42.1 ± 8.1 mM and 6.5 ± 3.0 μA mM^{-1} cm^{-2}, respectively. Repeated trials to determine

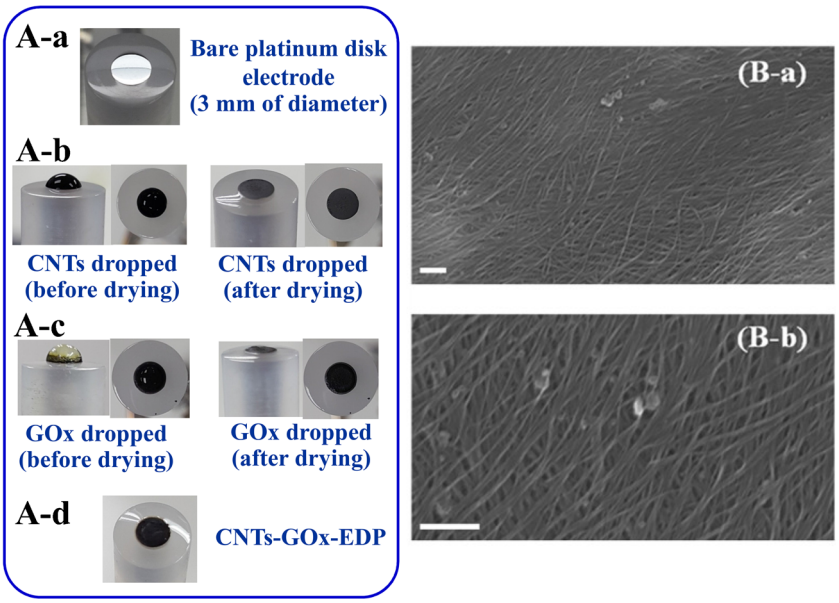

Fig. 1 Drop-and-dried carbon nanotube (CNT) electrode disk deposits. **A-a**, bare platinum disk electrode, of diameter 3 mm. **A-b**, placement of CNT deposits by drop-coating. **A-c**, loading of CNT layers with GOx by drop-coating. **A-d**, GOx/CNT surface layer after placement of a thin film of cathodic electrodeposition paint. **B-a** and **B-b**, dried CNT coating on a metal substrate surface: scanning electron microscope (SEM) images at two different magnifications. The white scale bars are 200 nm in length

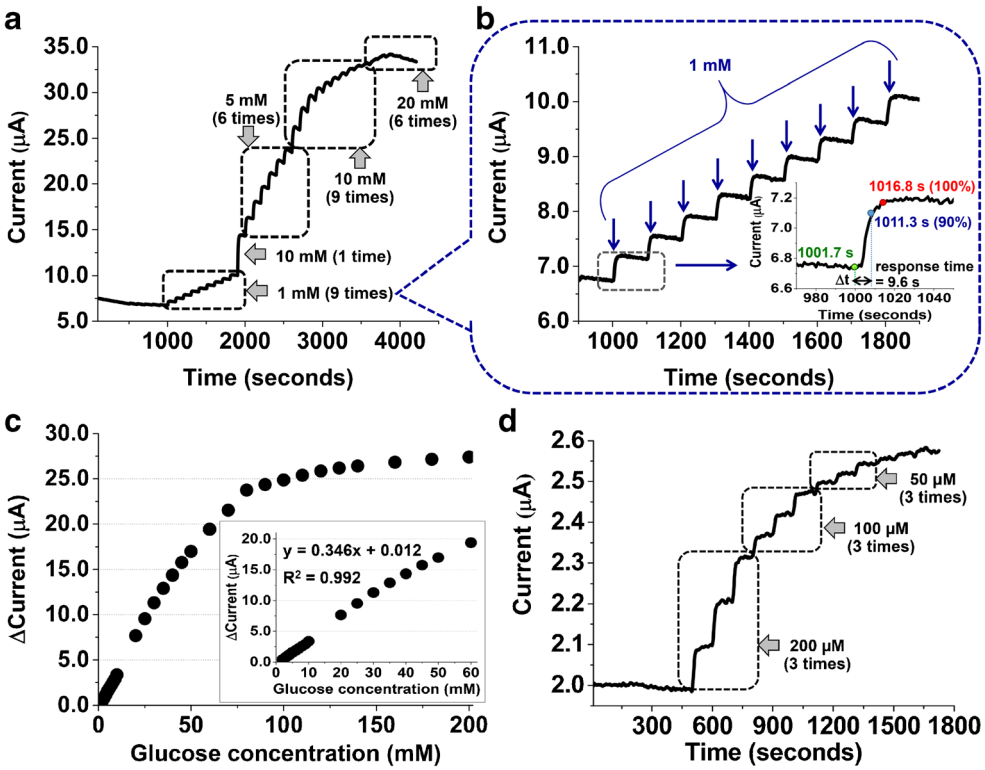

Fig. 2 (CNT-GOx) EDP-Pt glucose biosensor performance tests. **a**, representative i/t trace in a calibration trial, in which aliquots of glucose stock solution were added to stirred 0.1 M sodium phosphate, 0.1 M KCl (pH 7.0). The recording was made at the ambient temperature of 25 °C with a H_2O_2 detection potential of +0.6 V vs. Ag/AgCl. **b**, zoomed view of the initial section of the current trace in (**a**) and, inset, the response time estimation for the first of the 9 steps included in the zoom. **c**, calibration plot with data from the trace shown in (**a**); the inset shows the linear part of the calibration plot, with an R^2 of 0.992 or better. **d**, representative i/t trace, acquired with a (CNT-GOx) EDP glucose biosensor in evaluation of the practical detection limit

the practical detection limit showed that glucose additions to the measuring buffer as small as 50 μM produced analyzable stepped elevations of the faradaic biosensor signal (Fig. 2d). The effective working range for glucose quantifications was therefore approximately 0.05–40 mM.

Stability tests

A comparison of amperometric responses of sensors with and without the EDP topcoat verified the crucial role of the polymer glaze in glucose sensing. Calibrations were performed after overnight storage of completed sensors in buffer solution (0.1 M phosphate, 0.1 M KCl, pH 7.0), at 4 °C and after further 24 h storage. In the performance tests on days 1 and day 2 both (CNT/GOx)/EDP-Pt and (CNT/GOx)-Pt biosensors produced amperometric glucose calibration plots of the classic shape (Supplementary Fig. S2). However, the omission of the EDP apparently allowed diffusional loss of GOx from the matrix, resulting in a significant reduction in the anodic H_2O_2 current response and thus reducing the sensor's sensitivity. The lower observed dynamic range of EDP-free sensors reflects the lack of the external paint layer as barrier loss of immobilized GOx. (Supplementary Fig. S2A). The close similarity of the responses on days 1 and 2 for the EDP-coated glucose biosensor (Supplementary Fig. S2B) demonstrated, on the other hand, the ability of the electropaint layer to prevent the escape of GOx and maintain the signal stability.

Long-term maintenance of the response of leak-protected (CNT/GOx)/EDP biosensors was checked by prolonged use of a modified Au-disk version in an electrochemical flow cell. This showed the effect of continuous exposure to the hydrodynamic force of a stream of PBS through the small-volume compartment on the signals in repeated flow-based glucose calibrations. Prior to flow cell test runs CNT/GOx/EDP-Au biosensors were calibrated in a normal beaker-type electrochemical cell, after overnight refrigeration in phosphate/KCl and again after 6 days more of storage at 4 °C. After one-week of immersion in phosphate/KCl only a minor decrease in maximum biosensor current at saturation was detected, with an even smaller decrease in currents within the linear range (refer to Supplementary Fig. S3 for the calibrations on days 1 and 7).

Figure 3a shows a 200 h-long uninterrupted amperometric recording that followed the 'day 7' pre-calibration test and for the duration of which the CNT/GOx/EDP-Au biosensor was polarized to +600 mV *vs.* Ag/AgCl/3 M KCl and subjected to constant passage of buffer solution, either without or, in six calibration and two model sample analyses, with glucose at various concentrations. For the first four calibrations, and thus for about 94 h of flow operation, the response was maintained at virtually 100%; the signal then dropped to about 92% and 70% for the fifth (120+ h) and sixth (180+ h) calibrations, respectively.

A zoomed view of the CNT/GOx/EDP-Au biosensor signal in the flow cell at the fourth calibration is provided in Fig. 3b. Each increase in glucose level resulted a transient increase

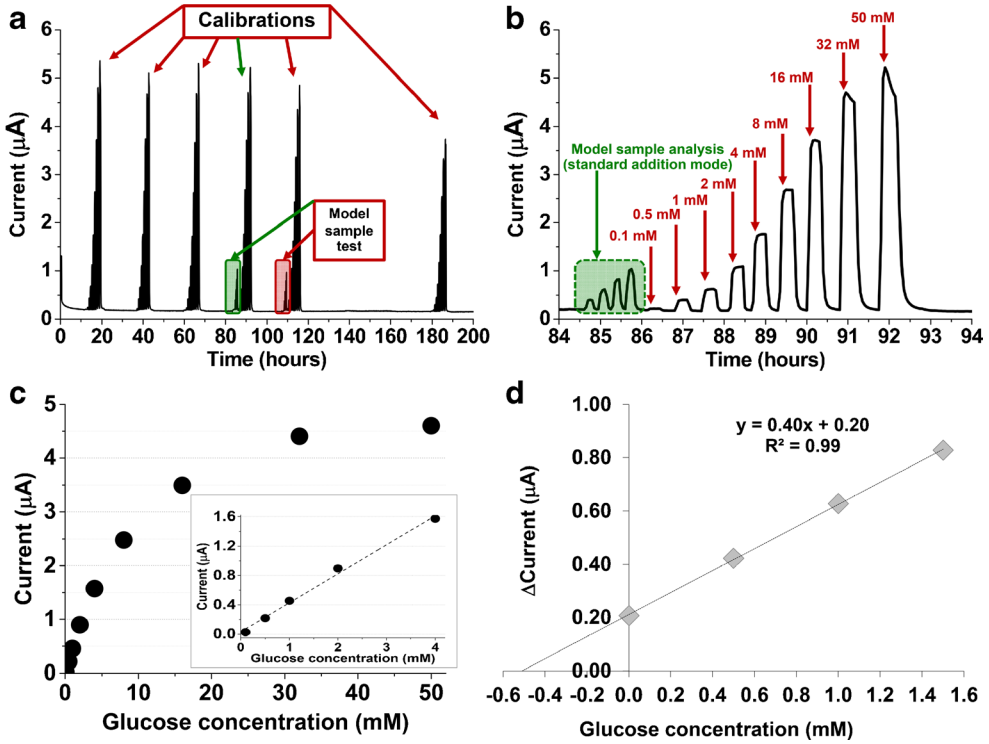

Fig. 3 Long-term stability measurements of CNT/GOx/EDP-Au biosensors. **a**, amperometric biosensor H_2O_2 current recording, including six calibrations and two model sample recovery tests, during continuous operation for about 200 h in an uninterrupted buffer stream through a three-electrode electrochemical flow cell. **b**, zoomed view of the 4th calibration and preceding 1st model sample recovery test. **c**, biosensor calibration plot computed from the original amperometry data of the 4th calibration, shown in (**b**). **d**, standard addition plot for the 500 μM model sample recovery test in (**b**). The running buffer throughout the trial was 0.1 M sodium phosphate, 0.1 M KCl (pH 7.0), passing through the tubing and electrochemical flow cell at 20 $\mu L/s^{-1}$. The amperometric biosensor was run at 25 °C with an anodic H_2O_2 detection potential of +0.6 V *vs.* Ag/AgCl

in the flow cell current and plots of maximum signal against glucose concentration showed typical Michaelis-Menten behavior, with an initial linear section followed by flattening of the curve as saturation was approached.

Consistent with the detection limit in beaker-type measurements, the lowest glucose concentration applied, 100 μM, generated a clear anodic H_2O_2 signal. However, the sensor currents at saturation (4.6 *vs.* 13.1 μA), linear range (4 vs. 40 mM) and sensitivity (5.4 *vs.* 2.5 μA mM^{-1} cm^{-2}) were not as close (Fig. 3c), the linear response range being smaller while the sensor sensitivity increased about twofold. The basis of these trends is unclear, but they may result from local hydrodynamics in the small dead-volume flow cell and related differences in the balance of diffusional and convectional glucose and/or molecular oxygen delivery to enzyme sites on the electrode, as compared to mass transport conditions in the stirred bulk of a large-volume container. Despite the reduction in the linear response range, CNT/GOx/EDP-Au biosensors performed well with samples of known glucose content, even after more than 100 h of continuous contact with the buffer stream. Assessment of a model sample (500 μM glucose) in standard addition mode, just before the 4th and 5th calibrations (84–86 and 108–110 h after the start of the trial), had satisfactory recovery rates of 102 and 100% (see Fig. 3d).

Glucose determinations in model and serum samples

CNT/GOx/EDP-Pt versions of the glucose biosensors were finally used for quantification of glucose in 0.1 M sodium phosphate, 0.1 M KCl (pH 7.0) with 10 mM glucose added to simulate an elevated plasma level, and for glucose determination in human serum, with a thin Nafion surface film placed on top to prevent interference by ascorbate and urate [29]. A hospital laboratory evaluation of 4.72 mM glucose for the serum sample served as reference. Supplementary Fig. S4-A and Fig. S4-C are the original biosensor current traces from standard addition mode trials on the model and real specimens, while Supplementary Fig. S4-B and Fig. S4-D are the resultant plots of signal *vs.* [glucose], showing glucose concentrations of 9.32 and 5.11 mM in the phosphate/KCl and serum samples, corresponding to recoveries of 93.2% and 108.3% respectively. Results of triplicate repetitions of the trial confirmed average determined glucose

concentrations in the model sample and serum, with standard deviations, as 9.66 ± 0.34 and 5.09 ± 0.09 mM, giving mean glucose recoveries of 96.6 ± 3.4% and 107.9 ± 1.8%, respectively (Supplementary Table S1). These recovery rates, well within the ±10% limit, indicated that CNT/GOx/EDP-Pt not only performed suitably in calibration trials but also can be practical tools for real sample glucose analysis.

In this study, the CNT/GOx/EDP-Pt biosensors were operated for glucose analysis at an anodic H_2O_2 detection potential of +600 mV *vs.* Ag/AgCl. At this amperometry layout the co-oxidation of blood ascorbic and uric acid at the sensing Pt disk is obviously a risk; however, adequate protection against the related signal disturbance, evidenced through the gain of a reasonable recovery of the glucose content of the shown serum sample analysis, was ensured through extra coverage of the functional sensor layer with a Nafion film and the ability of this negatively charged sensor surface modification to reject diffusional access of the interfering acid anions to the Pt electrode by effective electrostatic repulsion. Protection could of course also be gained through the choice of cathodic instead of the tried anodic sensing of enzymatically produced H_2O_2, but then at suitably electrocatalyst-modified electrode disks. A promising proof-of-principle amperometric calibration trial with CNT/GOx/EDP placements on Prussian blue (PB)-modified screen printed carbon electrodes (SPEs) revealed, for instance, that such a move from critical positive to favorable negative working potentials is indeed possible. Clear cathodic current steps were obtained with this configuration for sequential additions of glucose aliquots to measuring buffer (data not shown) and calibration plots indicated response linearity up to about 2 mM. The interference-free cathodic glucose analysis with the CNT/GOx/EDP-PB-SPE biosensor platform has yet to be optimized, as was done here for Pt disks equivalents with anodic detection, to tune this gentler signaling to best analytical performance.

Conclusion

CNT-based glucose biosensors with minimalistic sensing layer layout are achieved through simple drop/dry and electrodeposition of paint procedures and integration of glucose oxidase into a polymer-capped pure nanotube matrix. Wide linear range, low detection limit, good sensor lifetime and acceptable (serum) sample level recovery are competitive key performance characteristics, realized without supplementation of the immobilization layer with functional add-ons such as graphene, metal/metal oxide nanoparticles, chitosan, quantum dot or redox polymer. Cathodic electrodeposition paint worked well as the sensor layer coating, preventing leakage of the adsorbed enzyme.

Acknowledgements This work was supported by the Suranaree University of Technology (SUT) and the Office of the Higher Education Commission under NRU Project of Thailand through a SUT-PhD grant to WS and WR, Research Grant SUT1-102-52-24-01 to AS and budget allocations to AS and WS for maintenance of SUT's 'Biochemistry-Electrochemistry Research Unit'. Valued supplementary financial support came through budget allocations from SUT the Vidyasirimedhi Institute of Science and Technology (VISTEC) to Albert Schulte and Wipa Suginta. Sincere appreciation also goes to the company LHV Coatings Limited, Birmingham, England for kindly supplying the cathodic electrodeposition paint for research purposes and Dr. David Apps, quondam Reader, Edinburgh Medical School, University of Edinburgh, Scotland, for his critical manuscript reading and language improvements.

Compliance with ethical standards

The author(s) declare that they have no competing interests.

References

1. Heller A, Feldman B (2008) Electrochemical glucose sensors and their applications in diabetes management. Chem Rev 108:2482–2505. https://doi.org/10.1021/cr068069y
2. Wang J (2008) Electrochemical glucose biosensors. Chem Rev 108: 814–825. https://doi.org/10.1021/cr068123a
3. Rogers KR (2006) Recent advances in biosensor techniques for environmental monitoring. Anal Chim Acta 568:222–231. https://doi.org/10.1016/j.aca.2005.12.067
4. Kanyong P, Krampa FD, Aniweh Y, Awandare GA (2017) Enzyme-based amperometric galactose biosensors: a review. Mikrochim Acta 184:3663–3671. https://doi.org/10.1007/s00604-017-2465-z
5. Mano N, Edembe L (2013) Bilirubin oxidases in bioelectrochemistry: features and recent findings. Biosens Bioelectron 50:478–485. https://doi.org/10.1016/j.bios.2013.07.014
6. Azevedo AM, Prazeres DM, Cabral JM, Fonseca LPJ (2005) Ethanol biosensors based on alcohol oxidase. Biosens Bioelectron 21:235–247. https://doi.org/10.1016/j.bios.2004.09.030
7. Zhu C, Yang G, Li H, Du D, Lin Y (2015) Electrochemical sensors and biosensors based on nanomaterials and nanostructures. Anal Chem 87:230–249. https://doi.org/10.1021/ac5039863
8. Putzbach W, Ronkainen NJ (2013) Immobilization techniques in the fabrication of nanomaterial-based electrochemical biosensors: a review. Sensors 13:4811–4840. https://doi.org/10.3390/s130404811
9. Chen A, Chatterjee S (2013) Nanomaterials based electrochemical sensors for biomedical applications. Chem Soc Rev 42:5425–5438. https://doi.org/10.1039/C3CS35518G
10. Gupta S, Murthy CN, Prabha CR (2017) Recent advances in carbon nanotube based electrochemical biosensors. Int J Biol Macromol 108:687–703. https://doi.org/10.1016/j.ijbiomac.2017.12.038
11. Tîlmaciu CM, Morris MC (2015) Carbon nanotube biosensors. Front Chem 3:59. https://doi.org/10.3389/fchem.2015.00059
12. Yang C, Denno ME, Pyakurel P, Venton BJ (2015) Recent trends in carbon nanomaterial-based electrochemical sensors for biomolecules: a review. Anal Chim Acta 887:17–37. https://doi.org/10.1016/j.aca.2015.05.049
13. Barsan MM, Ghica ME, Brett CM (2015) Electrochemical sensors and biosensors based on redox polymer/carbon nanotube modified electrodes: a review. Anal Chim Acta 881:1–23. https://doi.org/10.1016/j.aca.2015.02.059
14. Zhu Z, Garcia-Gancedo L, Flewitt AJ, Xie H, Moussy F, Milne WIA (2012) A critical review of glucose biosensors based on

carbon nanomaterials: carbon nanotubes and graphene. Sensors 12: 5996–6022. https://doi.org/10.3390/s120505996
15. Jacobs CB, Peairs MJ, Venton BJ (2010) Review: carbon nanotube based electrochemical sensors for biomolecules. Anal Chim Acta 662:105–127. https://doi.org/10.1016/j.aca.2010.01.009
16. Luong JH, Male KB, Hrapovic S (2007) Carbon nanotube-based electrochemical biosensing platforms: fundamentals, applications, and future possibilities. Recent Pat Biotechnol 1:181–191. https://doi.org/10.2174/187220807780809427
17. Rivas GA, Rubianes MD, Rodríguez MC, Ferreyra NF, Luque GL, Pedano ML, Miscoria SA, Parrado C (2007) Carbon nanotubes for electrochemical biosensing. Talanta 74:291–307. https://doi.org/10.1016/j.talanta.2007.10.013
18. Gruner G (2006) Carbon nanotube transistors for biosensing applications. Anal Bioanal Chem 384:322–335. https://doi.org/10.1007/s00216-005-3400-4
19. Balasubramanian K, Burghard M (2006) Biosensors based on carbon nanotubes. Anal Bioanal Chem 385:452–468. https://doi.org/10.1007/s00216-006-0314-8
20. Lin Y, Yantasee W, Wang J (2005) Carbon nanotubes (CNTs) for the development of electrochemical biosensors. Front Biosci 10: 492–505
21. Wang J, Musameh M, Lin Y (2003) Solubilization of carbon nanotubes by Nafion toward the preparation of amperometric biosensors. J Am Chem Soc 125:2408–2409. https://doi.org/10.1021/ja028951v
22. Pumera M, Smid B (2007) Redox protein non-covalent functionalization of double-wall carbon nanotubes: electrochemical binder-less glucose biosensor. J Nanosci Nanotechnol 7:3590–3595. https://doi.org/10.1166/jnn.2007.846
23. Tsai YC, Li SC, Chen JM (2005) Cast thin film biosensor design based on a Nafion backbone, a multiwalled carbon nanotube conduit, and a glucose oxidase function. Langmuir 21:3653–3658. https://doi.org/10.1021/la0470535
24. Deng S, Jian G, Lei J, Hu Z, Ju H (2009) A glucose biosensor based on direct electrochemistry of glucose oxidase immobilized on nitrogen-doped carbon nanotubes. Biosens Bioelectron 25:373–377. https://doi.org/10.1016/j.bios.2009.07.016
25. Xue H, Sun W, He B, Shen Z (2003) Single-wall carbon nanotubes as immobilization material for glucose biosensors. Synth Met 135: 831–832. https://doi.org/10.1016/S0379-6779(02)00919-0
26. Gouveia-Caridade C, Pauliukaite R, Brett CMA (2008) Development of electrochemical oxidase biosensors based on carbon nanotube-modified carbon film electrodes for glucose and ethanol. Electrochim Acta 53:6732–6739. https://doi.org/10.1016/j.electacta.2008.01.040
27. Li J, Wang YB, Qiu JD, Sun DC, Xia XH (2005) Biocomposites of covalently linked glucose oxidase on carbon nanotubes for glucose biosensors. Anal Bioanal Chem 383:918–922. https://doi.org/10.1007/s00216-005-0106-6
28. Krylova I (2001) Painting by electrodeposition on the eve of the 21st century. Prog Org Coat 42:119–131. https://doi.org/10.1016/S0300-9440(01)00146-1
29. Spanu RA, Babudieri S, Latte G, Madeddu G, Galleri G, Nuvoli S, Bagella P, Demartis MI, Fiore V, Manetti R, Serra PA (2016) Enzyme biosensors for biomedical applications: strategies for safeguarding analytical performances in biological fluids. Sensors 16. https://doi.org/10.3390/s16060780